Decision Fusion-Based Non-Intrusive Load Identification Involving Adaptive Threshold Event Detection

Yaqian Huang, Yanqing Zhu, Jingyi Pan, Yunpeng Gao, Fenghua Peng, Yichuang Sun

***Abstract*—Non-intrusive load monitoring (NILM) is an important measure to improve the intelligence level of the power demand side. Existing NILM methods have poor performance in identifying low-power devices with similar power, with the increasing diversity of household loads and the wide range of load fluctuations. This paper proposes a fusion-based load identification method for residential loads, considering the electrical characteristics of different load types. In the first stage, the adaptive threshold Cumulative Sum (CUSUM) algorithm is innovatively adopted to reduce the misjudgment of local high-power device switching fluctuations and the missed events of local low-power load operation in the global threshold. In the second stage, the minimum Bayesian decision fusion loss function is used to calculate the cost function of Voltage Current (UI) trajectory, power, and total harmonic distortion, which are input into the Softmax multi-classification regression model in parallel. The category corresponding to the prediction made by the minimum loss function is considered as the final output. Finally, the effectiveness of the proposed method in identifying multiple types of household loads was verified through experiments on the Plug-Level Appliance Identification Dataset (PLAID) dataset.**

***Index Terms*—Non-intrusive load monitoring, event detection, load identification, decision fusion.**

I. INTRODUCTION

WITH the development of smart grid, there is an increasingly urgent need to promote efficient electricity utilization and optimize electricity usage patterns to strengthen the management of electricity consumption in the whole society, which necessitates an accurate understanding of energy consumption on the load side. Non-intrusive load monitoring (NILM) can be based on the electricity consumption information of the total load table, and obtain the specific load status mode and electricity consumption level of a single device through appropriate software analysis methods to help users and energy suppliers allocate power resources more reasonably, particularly in the context of demand response [1]. It is an important measure to improve the intelligence level of the power demand side [2]. For energy suppliers, gaining access to refined data regarding the load side enables accurate estimation of total electricity consumption on a macro scale. This information is instrumental in implementing sophisticated electricity policies, including time-of-use pricing, which can help balance supply and demand dynamics more effectively.

Currently, NILM encompasses two main methodologies: event-based and non-event-based methods. Non-event-based methods often treat the state of appliances as variables, utilizing pattern recognition techniques to match various appliance states and powers with the total power sequence. This includes direct decomposition of load power using various deep learning algorithms, among other approaches[3][4]. However, non-event-based methods tend to be slower and may not be suitable for scenarios with a large number of appliances[5]. Event-based methods consist of three steps: event detection, feature extraction, and load identification[6]. This method incorporates feature extraction into the event detection process, initially determining the time point of the transient and steady-state division where load switching occurs, and then extracting features, which can better capture transient features and enrich the diversity of recognition features.

Existing event detection methods can be categorized into three classes: heuristic event detection, matched filtering, and probability model-based detection[7]. The heuristic method relies on prior knowledge to establish event detection rules. For example, the earliest type of heuristic event detection method was proposed by Hart[8], which compares power difference changes with a predefined threshold to determine event occurrence points. However, the effectiveness of this approach is often limited in scenarios with diverse types of household loads and significant amplitude fluctuations[9].The matched filtering method involves comparing the signal to be detected with pre-established library signals using correlation methods to locate load switching events. However, experiments have shown that this type of method can be cumbersome when applied to the detection of multiple load categories[10][11]. Moreover, it is susceptible to interference from noise and other factors. Therefore, in the scenario of household loads, the accuracy of matched filtering method does not have a significant advantage. The probability model-based method is currently the most widely used[12][13],

This work was supported by the National Key Research and Development Program of China under Grant2021YFF0602402. (Corresponding author: Yanqing Zhu.)

Yaqian Huang, Yanqing Zhu, Jingyi Pan and Yunpeng Gao are with the College of Electrical and Information Engineering, Hunan University, Changsha, Hunan 410012, China (e-mail: 2500678053@qq.com; zyq@hnu.edu.cn; 1052531295@qq.com; gaoyp@hnu.edu.cn).

Fenghua Peng is with State Grid Hunan Electric Power Company Ltd., Changsha, Hunan 410000, China (e-mail: 34585804@qq.com).

Yichuang Sun is with the School of Engineering and Technology, University of Hertfordshire, AL10 9AB Hatfield, U.K. (e-mail: y.sun@herts.ac.uk).

which focuses on the changes in statistics in the total load data to locate the time of load changes. Representative methods in this category include the goodness-of-fit method, cumulative sum (CUSUM) algorithm, likelihood ratio test, etc. Among them, the CUSUM algorithm is the most widely used[13][14]. The bilateral CUSUM algorithm based on sliding window was proposed and applied to event detection [13]. The CUSUM algorithm was applied based on statistical features such as variance and absolute deviation in the sampled total signal, using a sliding window method to determine the moments of load switching [12]. Currently, there have been no improvements to the CUSUM algorithm specifically addressing the problem of misjudgment caused by fluctuations in local high-power devices and the issue of missing events in the operation of local low-power loads in household loads. Therefore, an adaptive threshold CUSUM algorithm is proposed to solve this problem.

Initially, active power was widely used for feature extraction due to its accessibility, but its sole reliance proved inadequate for identifying increasingly diverse load types [15]. The Voltage Current (UI) trajectory features, with their rich representation forms and graph structure transformation advantages, have been widely applied, yielding satisfactory results [16]. However, relying solely on UI trajectories often leads to suboptimal load identification within the same class, as trajectory shapes of the same electrical type are similar. Harmonics, capturing the characteristics of power electronic devices, are now incorporated as non-intrusive load identification features, offering auxiliary characteristics for enhancing accuracy. Harmonic features are peculiarities that electronic devices have in terms of the distribution and magnitude/amplitude of the current harmonic spectrum, even in the absence of voltage harmonics. Amplitude of odd harmonics and harmonic ratio are adopted as load features to improve identification precision [17][18]. Researchers have started investigating feature fusion methods to address load feature selection, mainly focusing on feature layer fusion [19][20]. For instance, UI trajectories and power features are fused to form composite features, and spectral envelopes serve as harmonic supplementary features [21]. However, there's currently no method effectively combining load types and characteristic features to optimize identification performance. Therefore, in diverse household load scenarios, UI trajectory, power, and Total Harmonic Distortion (THD) are selected as distinctive load features based on their distinguishing attributes.

For load identification, three main methods are prominent. The first involves establishing relevant load models and using model matching techniques. Hidden Markov models are favored by some researchers for their ability to learn and match optimal state sequences based on observed load parameters [22]. The second method is seeking optimal solutions by constructing a graph signal model from the overall sampled load signal. Power constraints are derived from the graph signal model, with alternating optimization and automatic adjustment of regularization coefficients aiding load category discrimination [23]. The third method harnesses neural networks and deep learning approaches such as convolutional neural networks [24], deep belief networks [25], Recurrent Neural Network (RNN) models [26], Long Short-Term Memory (LSTM) [27] and Gated Recurrent Unit (GRU) [28]. Selecting the most suitable load identification algorithm with the right balance of complexity and accuracy is a key focus in practical applications, leading to the proposal of a decision fusion method based on Softmax-Bayesian.

This paper proposes a non-intrusive load identification method that innovatively combines an adaptive threshold CUSUM algorithm with Softmax-Bayesian decision fusion. This pioneering approach fills the blank in previous studies. Also, identifiable load features are selected according to the characteristics of load types in scenarios with a wide variety of household loads, based on the diversity of load characteristics and the local similarity of electrical features exhibited by different types of loads. The primary contributions of this study are as follows:

1) An adaptive threshold CUSUM event detection method is proposed to address the problem of misjudgment for high-power events and missed detections for low-power events caused by the large range of power spans in existing change-point detection theory.

2) A non-intrusive load identification method based on decision fusion Softmax Bayesian is proposed, which solves the limitation of inaccurate identification of some components when using a single load feature.

3) The combination of an adaptive threshold CUSUM algorithm with Softmax-Bayesian decision fusion is employed to achieve higher performance. Experimental results demonstrate that using this approach for load identification of seven common household appliances yields an average F1-score of 0.97. This significantly improves the accuracy of identifying loads.

II. METHODS

A. CUSUM Event Detection Method Based on Adaptive Threshold

In non-intrusive load identification algorithms, event detection is a crucial step in obtaining the time of event occurrences and extracting load features. The time list of load event occurrences can facilitate the extraction of subsequent transient steady-state load features, forming a rich load feature library.

In order to address the issue of large fluctuations in load events, a challenge arises when using power as the feature for event detection. The identification performance of high-power and low-power events is often hindered due to the setting of the threshold. To overcome this challenge, a binary search method is proposed, with relatively low identification accuracy but simple algorithm principle for preliminary and rapid partitioning of the load power range to determine sub-interval thresholds. Then, the CUSUM algorithm is combined

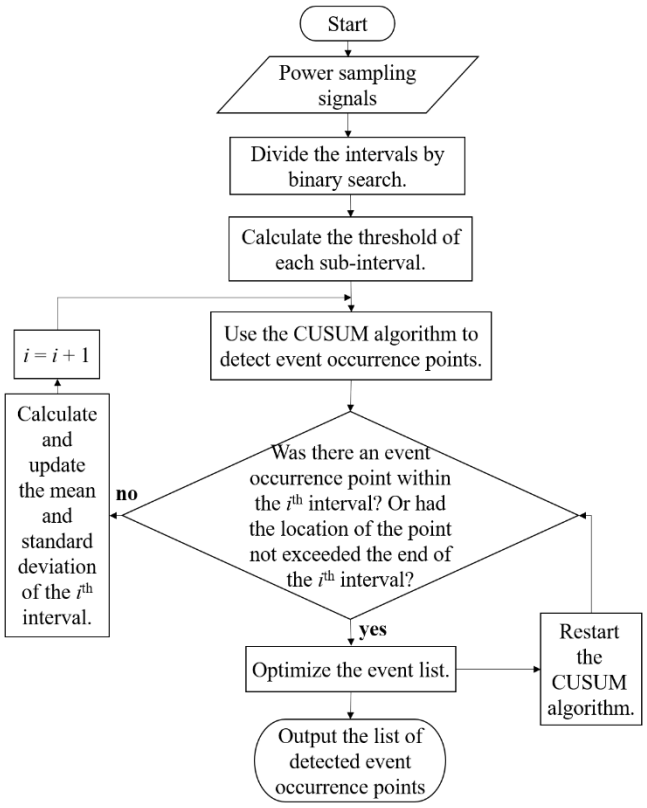

Fig. 1. Flow chart of adaptive threshold CUSUM event detection.

with higher complexity but higher identification accuracy to perform the final load event detection, using locally partitioned thresholds for detection[29]. This approach follows the Pauta Criterion to form sub-interval thresholds, reducing the risk of false alarms caused by fluctuation of high-power devices in the global threshold and preventing the missed detections of events related to low-power load operations.

The flowchart of the event detection method is shown in Fig. 1. Firstly, input the power sampling signals. Then divide the intervals by binary search, calculate the means and variances of the intervals and obtain a list of sub-interval means and variances. Subsequently, calculate the threshold of each sub-interval using the Pauta Criterion. Next, use the mean and standard deviation of the $(i\text{-}1)^{th}$ interval as the threshold for the i^{th} interval. Apply the CUSUM algorithm to detect event occurrence points. Determine if there was an event occurrence point within the interval or if the location of the point had not exceeded the end of the i^{th} interval. If Yes, apply peak finding and derivative to optimize the event list. Shift the point forward by $0.2*f1$ transient intervals and restart the CUSUM algorithm. If no, calculate and update the mean and standard deviation of the i^{th} interval, increase the value of i by 1. Finally, output the list of detected event occurrence points.

The essence of the binary search method is to calculate the sum of the loss functions on both sides of any given point and identify the point that minimizes this sum as the first change point[30]. Subsequently, the time series signal is divided into two segments at the first change point, and the first step is

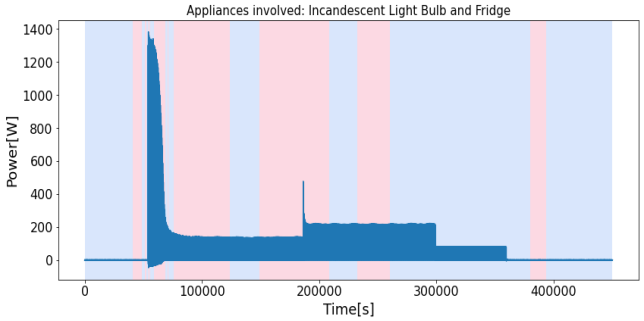

Fig. 2. Results of binary search coarse detection division.

repeated for each segment until the termination condition is satisfied, after which the detection stops and outputs the change points. The expression for the binary search method is shown in (1), where t_1 denotes the first change point, $c(y_{0.....t_1})$ denotes the value of the loss function from time point 0 to t_1, and $c(y_{t_1.....T})$ denotes the value of the loss function from t_1 to the end of the time series signal T.

$$t_1 = \operatorname{argmin}_{0<t<T}\left\{c(y_{0.....t_1}) + c(y_{t_1.....T})\right\} \tag{1}$$

In (1), the value of c can be calculated by selecting an appropriate loss function. The loss function C_{linear}, based on the least squares criterion, represents the residual sum of squares between the actual signal and the fitted model signal. The expression for C_{linear} is shown in (2), where $y_{a...b}$ refers to a subsequence of the sequence y, which starts from index a and extends to index b, y_t denotes the observed value of the signal at time point t, u and v denote the unknown regression parameters, $x_t^{'}$ and $z_t^{'}$ denote the observed covariate subsegments, R denotes the set of real numbers. C_{linear} is primarily used to measure errors. The optimal loss function C_{linear} is ultimately chosen as the loss function for the binary search method to determine the initial interval threshold during coarse detection.

$$C_{\text{linear}}(y_{a...b}) = \min_{u\in \mathrm{R}, v\in \mathrm{R}} \sum_{t-a+1}^{b} (y_t - x_t^{'}u - z_t^{'}v)^2 \tag{2}$$

Since the number of load events within a sampling time period cannot be determined in advance, the termination condition for the loop is selected to utilize a penalty constraint mechanism Pen as shown in (3), where p denotes the dimension of the signal, representing the number of distinct features or parameters being measured or analyzed within the signal, T denotes the length of the signal sequence, indicating the total number of data points or observations captured over a specific time span, and τ denotes the number of the change points.

$$Pen = \frac{p}{2} * \log(T) |\tau| \tag{3}$$

Based on the aforementioned application of binary search to the sampled load power time series, an initial detection of time change point coordinates is outputted, dividing the sampled load power signal into several sub-intervals of transient steady states. By selecting the appropriate loss function and penalty constraint mechanism, this method can effectively converge and complete the division of interval. The graphical representation is shown in Fig. 2, where the light blue and red

boundary regions represent the intervals divided by the binary search method, and the deep blue region represents the original load power sequence to be detected.

According to the Pauta Criterion in statistics, assuming that the load data follows a normal distribution or an approximately normal distribution, it indicates that there is a probability of 0.9974 that the data falls within the range of (μ-3σ, μ+3σ), where μ represents the mean, and σ represents the standard deviation.

After partitioning the intervals, each interval will have a constant mean and variance. Based on this, we can calculate the mean and variance of each sub-interval. Therefore, by selecting an upper threshold value, denoted as 3σ, and a lower threshold value, denoted as -3σ, results obtained from the binary search method can be stored. These stored values will be used for determining the thresholds in the current stage and passed into the next stage, which is the adaptive threshold detection part of the fine detection CUSUM algorithm.

The decision formula for the bilateral CUSUM detection algorithm is shown in (4) and (5), where x_k denotes the observed value of the k^{th} point, g_k^+ and g_k^- denote the forward cumulative sum and the backward cumulative sum of the k^{th} point, μ_0 denotes the mean value of the monitoring signal and β denotes the allowable noise fluctuation error. Based on (4) and (5), the value of μ_0 is updated with the previous sub-interval obtained through the binary search method. Assuming that the mean value sequence of k sub-intervals detected by the binary search method in the signal sequence is $\mu=\{\mu_0,\mu_1...\mu_k\}$, and the standard deviation of the k sub-intervals is $\sigma=\{\sigma_0,\sigma_1...\sigma_k\}$.If $\mu_0\neq\mu_1$, it indicates that a change point exists in the first interval, and the CUSUM algorithm needs to be invoked within the first sub-interval. The mean value μ_0 of the zeroth interval is used as the mean value in the first sub-interval, and according to the Pauta Criterion, the mean value σ_0 of the zeroth interval is constructed as 3*σ_0 to form the detection threshold for the first sub-interval.

$$g_k^+=(g_{k-1}^+ +x_k-\mu_0-\beta) \tag{4}$$

$$g_k^-=(g_{k-1}^- -x_k+\mu_0-\beta) \tag{5}$$

After the change point is detected in the first sub-interval, firstly the mean and standard deviation of the first sub-interval should be updated. Starting from the steady-state moment when the event time change point is detected, the normalized transient interval is set as 0.2s, assuming the sampling frequency of the dataset is f_1. Converting it to coordinate representation, it becomes 0.2*f_1. Therefore, the CUSUM algorithm should move the steady-state interval coordinates forward after detecting the first change point in this sub-interval. Calculate the mean and standard deviation from the steady-state interval to the end of the first sub-interval, and update μ_1 and σ_1 accordingly. Then, repeat the same operation for all subsequent sub-intervals to complete the threshold update and event detection using the CUSUM algorithm.

B. Feature Extraction and Database Construction based on Event Time List

The types of loads include resistive loads, power electronic loads, and motor-driven loads. UI trajectory features can be used to identify and effectively differentiate most devices. However, for the above three types of loads, power features provide a simple and rapid way to distinguish most devices. Nevertheless, in the case of similar low-power consumption power electronic loads within the same category, harmonic characteristics serve as a robust supplementary feature for load identification. Therefore, to achieve effective recognition of the aforementioned household load types, UI trajectory, power, and THD are selected as three features for load identification.

Based on the load event occurrence point t_k, a steady-state current I_1 is sampled for one cycle before t_k, and a steady-state current I_2 is sampled for one cycle after t_k. The steady-state current I_{event} corresponding to each individual occurrence point is obtained by subtracting I_1 from I_2, and the steady-state current I_{event} is subjected to Fourier Transform to obtain each harmonic current I_k. The Fourier Transform operation is shown in (6), which converts the current periodic signal into a set of DC components and sine waves with different frequencies, amplitudes, and phases, thus obtaining information about the harmonic currents[31]. Based on the harmonic information, the order of harmonics and total harmonic distortion of the current are obtained. The calculation of the *THD* for each event occurrence time is as defined by (7), and the *THD* dataset is constructed based on the event labels[32].

$$I_k=a_1\sin(\omega t+\theta_1)+\ldots+a_k\sin(k\omega t+\theta_k) \tag{6}$$

$$THD=\frac{\sqrt{\Sigma_2^n {I_n}^2}}{I_1} \tag{7}$$

By subtracting the steady-state current I_1 sampled for one cycle before the load event occurrence point t_k from the steady-state current I_2 sampled for one cycle after t_k, the current value I_{event} for a single event operating for one cycle in a stable manner is obtained. Multiplying the current value I_{event} by the voltage value U gives the power value for the load event's operation, as expressed by (8).

$$\Delta p=I_{\text{event}}*U \tag{8}$$

The UI trajectory curve is a typical feature proposed in recent years for electrical load classification [18]. It represents a two-dimensional load feature. The construction of UI trajectory features is derived from the steady-state voltage and current characteristics of the load within one cycle.

Based on the principle of UI trajectory features, the establishment of the UI trajectory feature library mainly involves three steps: extracting the steady-state current of the load within one cycle, extracting the steady-state voltage of the load, and normalizing the data.

C. Load Identification Based on Softmax-Bayesian

The time list of load event occurrences facilitates the extraction of transient load features, leading to a rich load feature library. Building upon this foundation, this paper

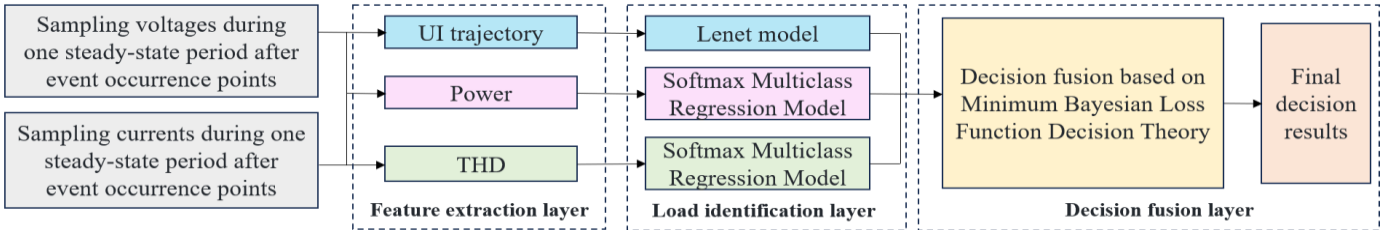

Fig. 3. Flowchart of load identification based on Softmax-Bayesian fusion model.

proposes a load identification framework based on the Softmax-Bayesian fusion model. This framework aims to enhance the accuracy of identifying different household load categories by leveraging the complementary advantages of various load features. The flowchart of the identification process is illustrated in Fig. 3.

In the output layer of the Softmax multiclass regression model, there are seven neurons corresponding to seven probability outputs, representing the probabilities of predicting each category. The probabilities of all categories in the output layer sum up to 1. y_1,y_2,y_3,y_4,y_5,y_6 represent the specific output probabilities for each category. The operations between each layer in the model still follow the pattern of linear regression, which essentially involves matrix-vector multiplication to linearly transform the feature space from one to another. The mathematical expression for this operation is shown in (9), where x_1,x_2 denote the input features, ω_1,ω_2 denote the weights to be learned, and b denotes the biases.

$$Out=\omega_1*x_1+\omega_2*x_2+b \tag{9}$$

In the Softmax regression model, after the linear operations between layers mentioned above, a Softmax operation is applied to the output layer. This operation transforms the model's outputs into corresponding probability values within the range of (0,1). The model structure diagram is shown in Table I, each layer within the model processes input data through various operations and passes the result to the next layer, output shape describes the shape of the result outputted by each layer after data processing, and param refers to the weights and biases learned by the model during the training process. The output layer contains six neurons represented as O_1. The final output is denoted as y_1. With this operation, the Softmax multiclass regression model becomes more suitable for predicting and operating with discrete values.

Based on the electrical features of different load types, three representative load features, namely UI trajectory, power, and THD, are simultaneously inputted into the Softmax multiclass regression model and the Lenet model for load type identification. This process generates three local decisions based on the three types of features. These three local decisions are then passed to the load identification fusion decision layer, where the minimum Bayesian loss decision function is employed for decision fusion.

The minimum Bayesian loss function decision fusion method [33] is introduced, which is grounded in Bayesian decision theory. This method primarily emphasizes the multiplication rule during the process of classifier fusion, integrating decision probability values from each classifier with local decision loss functions. The decision loss functions for each classifier are formulated based on the probabilities of sample classes in the training dataset and the associated loss for correct and incorrect decisions. For binary classification, the fusion rule's loss function is depicted in (10), where P_0 and P_1 denote the probabilities of the first and second class samples respectively. $P(d=H_0/H_0)$ represents the probability that a sample belongs to the first class and is correctly predicted by the classifier, while $P(d=H_1/H_0)$ denotes the probability that an actual first-class sample is erroneously predicted as belonging to the second class. Additionally, c_{01} signifies the loss associated with the erroneous prediction of a first-class sample as belonging to the second class, and c_{10} represents the loss associated with the erroneous prediction of a second-class sample as belonging to the first class. The total loss function incorporates these probabilities and losses to provide a comprehensive measure of the fusion method's performance.

$$\begin{aligned} C(d,H)=&P_0c_{00}P(d=H_0/H_0)+P_0c_{10}P(d=H_1/H_0)\\ &+P_1c_{01}P(d=H_0/H_1)+P_1c_{11}P(d=H_1/H_1) \end{aligned} \tag{10}$$

Before being passed to the fusion decision layer, the value of $P_iP(d=H_j/H_i)$ can be already determined based on the confusion matrices from the local decision process and the distribution of the sample set. Then $P_iP(d=H_j/H_i)$ is uniformly denoted as K_{ij}. K_{ij} represents the probability that a sample actually belongs to class j, but is predicted to belong to class i. Therefore, (10) can be transformed into (11).

$$C(d,H)=\sum_{i=0}^{n}\sum_{j=0}^{n}K_{ij}c_{ij} \tag{11}$$

Finally, the designed experimental process for the minimum Bayesian loss function decision fusion method is as follows:

Step 1: Since three distinct and representative load features are utilized, the classifier models are trained by incorporating these features based on their characteristics. This training process yields three confusion matrices, denoted as CM_1, CM_2, and CM_3. The sample class probability distribution matrix P_i of the confusion matrices is multiplied to obtain the corresponding model recognition performance matrices PM_1, PM_2, and PM_3, as shown in (12).

$$PM_k=P_i\times CM_k \tag{12}$$

Step 2: For each sample i, after the three features are extracted and identified by the models, three corresponding load identification results, denoted as d_1,d_2,d_3, are obtained. Thus, based on $c_{ij}=\sum_{j=1}^{n}\left|d_j-d_{H_i}\right|$, the distance losses of each model for each sample are calculated, resulting in $c_{ij(1)}$,$c_{ij(2)}$,$c_{ij(3)}$. The target value of the sample, denoted as d_{H_i}, is represented as 1 for the probability value corresponding to

TABLE I
STRUCTURE OF SOFTMAX MODEL

Softmax_model architecture		
Layers	Output Shape	Parameters
flatten_1(Flatten)	(None, 1)	0
dense_4 (Dense)	(None, 48)	96
dense_5 (Dense)	(None, 24)	1176
dense_6 (Dense)	(None, 12)	300
dense_7 (Dense)	(None, 7)	78
Total Parameters: 1650	Trainable Parameters: 1,650	Non-Trainable Parameters: 0

TABLE II
COMPARISON OF EXPERIMENTS

	F1-Score	False	Hausdorff distance
Fixed threshold(25W)	0.178	19937.9	79679.9
Fixed threshold(150W)	0.287	21.4	90822.4
Adaptive threshold	0.866	2.1	10605

the target category, and 0 for the probability values corresponding to all other categories.

Step 3: Based on the model recognition performance matrices, K_{ij} is calculated. By multiplying according to (11), the loss functions $C_1(d,H_i)$, $C_2(d,H_i)$, and $C_3(d,H_i)$ for each model regarding sample i are obtained.

Step 4: The final decision fusion result is determined by selecting the minimum value among the cost loss functions of the three classifier models. In this step, the process of decision fusion is completed.

III. EXPERIMENTAL RESULTS AND ANALYSIS

A. Experimental Verification of Adaptive Threshold CUSUM Event Detection

The total sampling dataset from the PLAID dataset consists of 500 turn-on time files, each containing 4 event occurrences. For a total of 2000 true event points, the fixed threshold CUSUM algorithm and the proposed adaptive threshold detection method combining binary search and CUSUM algorithm are compared in terms of evaluation metrics, as shown in Table II. The false positive rate metric is calculated as the mean error from each file. The Hausdorff distance quantifies the maximum distance from any point in one set to its nearest point in the other set, and it is utilized to assess the similarity or dissimilarity between two images or objects.

Due to the combination of binary search and CUSUM algorithm in the adaptive threshold event detection method based on intervals, most change points are detected earlier compared to the actual change points. While they are close to

TABLE III
COORDINATE COMPARISON OF EVENT DETECTION

File 10 real switching points	File 10 detected switching points	File 2 real switching points	File 2 detected switching points
35353	31615	47764	44261
91346	91748	107632	107587
175750	174663	224097	224830
233571	232425	281983	281963

TABLE IV
SUMMARY OF 7 ELECTRICAL APPLIANCES

Load identifiers	Load types	Power	Harmonics	UI trajectory
0	CFL	15W-30W	Substantial Odd Harmonics	
1	hairdryer	250W-1200W	Minor Third Harmonics	
2	electric kettle	800W-1500W	None	
3	laptop	15W-50W	Substantial Odd Harmonics	
4	electric fan	20W-100W	Minor Third Harmonics	
5	microwave oven	300W-600W	Substantial Odd Harmonics	
6	vacuum cleaner	400W-1100W	Minor Third Harmonics	

the change point intervals and the difference is not significant, factors such as transient intervals and the initial partitioning of the binary search contribute to a slight distance between the detected change point positions and the actual coordinates. These nuances are further elucidated through the comparison of event detection coordinates as depicted in Table III.

Based on the aforementioned metrics, the proposed adaptive threshold CUSUM algorithm achieves an improvement in the F1 score, which reflects the accuracy of event detection, to 0.866. This statistical result is based on 2000 true event points. It demonstrates that this method exhibits better robustness for detecting opening events with different magnitudes.

B. Experimental Verification of Decision Fusion Load Identification Method

To verify the effectiveness of the proposed algorithm in load identification, the publicly available PLAID dataset is used for experimentation. The PLAID dataset is obtained from real sampling among household users and covers common resistive loads, motor-driven loads, and power electronics loads. The PLAID public dataset comprises voltage and current data samples, obtained at a frequency of 30 kHz during the summer of 2013 from 56 households in Pittsburgh, Pennsylvania, USA[34]. It encompasses recordings from 8 different appliance types, with each type consisting of 3-6 sets of load data from various models and brands. Records with significant noise in the PLAID dataset are eliminated, resulting in a final dataset of 1094 sampled instances. The PLAID dataset includes aggregated and disaggregated data.

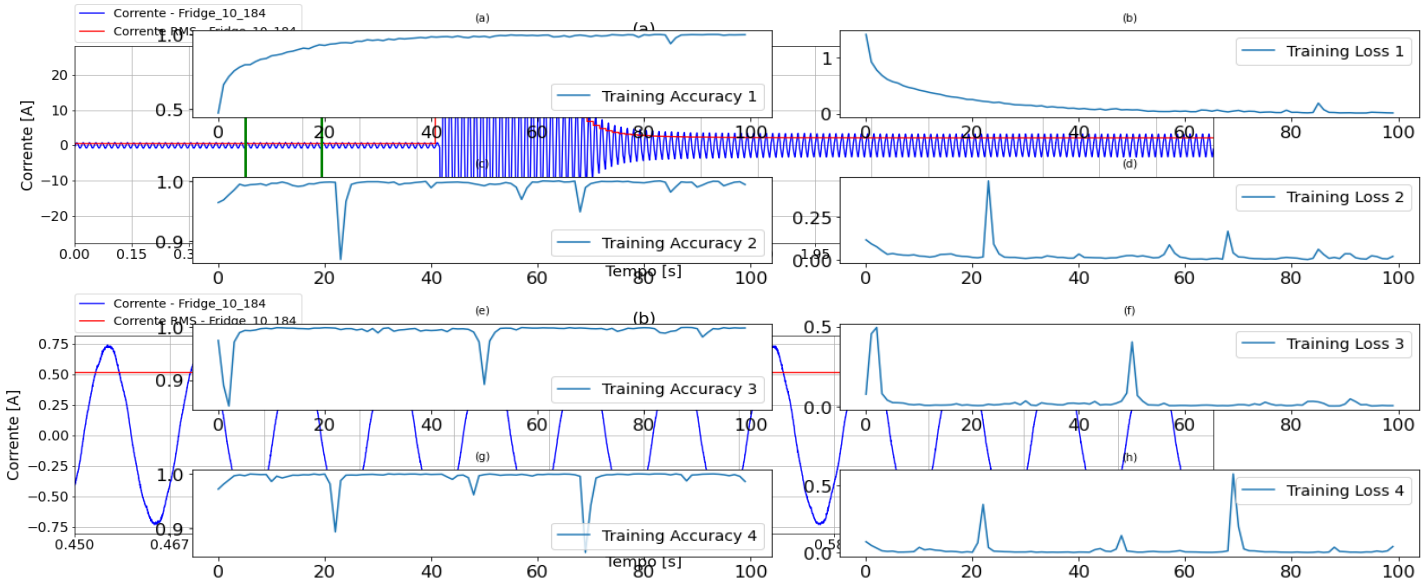

Fig.4. Current waveform of refrigerator when operating.

The aggregated data consist of high-frequency samples collected when two or more appliance loads operate simultaneously. These records are labeled with event occurrence timestamps and specific load category operation labels, facilitating model learning and training. An illustrative example is the current waveform graph sampled from the disaggregated refrigerator-end data, as depicted in Fig.4. In (a), the graph represents the current signal, with the green line in (a) denoting an extracted steady-state period shape. In (b) it illustrates the current waveform when the appliance operates independently.

In the context of household use, the diversity of household electrical appliances is steadily increasing, with an ordinary household often comprising a dozen of appliance types. However, loads with similar operational principles and physical structures tend to exhibit comparable electrical characteristics. Table IV has been compiled summarizing seven common household appliances, including Compact fluorescent lamp (CFL), hairdryer, electric kettle, laptop, electric fan, microwave oven, and vacuum cleaner, detailing the features of each, and assigning them identifiers ranging from 0 to 6.

The experimental verification consists of two parts. The first part is the load category discrimination experiment completed by fusing local decisions through the minimum Bayesian loss function. The second part is to compare the experimental results with other methods that use the PLAID dataset in existing references, further verifying the effectiveness of the proposed multi-decision fusion load identification method.

The features were extracted from seven different types of appliances mentioned before. For each type of appliance, 200 samples of different brands and models were collected, totaling 1400 samples. During the feature extraction process, voltage and current signals during appliance operation were first recorded for each sample. Subsequently, signal processing techniques such as harmonic analysis and power calculation were employed to extract THD, power, and UI trajectory features from these signals. These features reflect the performance and characteristics of appliances under various operating conditions, providing crucial data foundation for training the load identification model. Finally, three input datasets were utilized, each containing 1400 feature samples, serving as the training dataset. The Lenet model was used for training the UI trajectory features. The cross-entropy loss function was selected as the loss function, and the Adam optimizer was used[35]. The number of iterations was set to 100. Pre-training was conducted using the MINIST publicly available dataset. After training, a fully connected layer with the activation function Softmax was concatenated as the final output model for prediction. Additionally, the UI trajectory images were normalized to a size of 128*128 to further improve the convergence speed of the model[36][37].The training effect of the Lenet model is shown in Fig.5. After pretraining with the Lenet model on the MINIST dataset, training convergence and achieved satisfactory performance have been observed, indicating that the model has acquired the capacity of a universal classifier.

The THD and power difference features were trained using a Softmax multi-classification model. The Adam optimizer was employed, and the cross-entropy loss function was utilized. During the training of power difference features, the model was iterated for 100 epochs, with the loss function calculated throughout the iteration process[35]. The model with the lowest loss function was selected for the prediction of THD and power difference features.

To validate the effectiveness of the Softmax-Bayesian decision fusion load identification method, a more diverse range of load types was adopted to closely resemble the load identification scenario in actual household settings. For each type of load devices, two to three representative household appliances were selected. The data used for sampling was

obtained from actual samples collected from residential users.

Fig.5. Training accuracy_loss iteration of the Lenet model.

The experimental model structures and training parameters remained consistent with the previous section. Firstly, each individual feature was inputted into the model in parallel for training to obtain local decision results. Subsequently, the Bayesian decision fusion was applied by minimizing the loss function to obtain the corresponding final decision fusion results.

The confusion matrix for the recognition of the seven types of devices under the THD feature input model is shown in Fig. 6. In the figure, the categories 0, 1, 2, 3, 4, 5, 6 represent incandescent lamp, CFL, electric fan, hair dryer, laptop, microwave oven, and vacuum cleaner, respectively. According to the results displayed in the confusion matrix, the THD feature exhibits good recognition performance for incandescent lamps and laptops, with the majority of instances being correctly identified. The THD feature shows the worst recognition effect on fans, possibly due to the special motor contained in its structure, which generates complex harmonic components. As mentioned earlier, incandescent lamps belong to resistive devices, while laptops belong to power electronic devices, representing two different types. During operation, incandescent lamps do not generate harmonics, while laptops generate a large number of odd harmonics. In this case, the harmonic feature proves to be effective in distinguishing between these two categories.

The confusion matrix for the recognition under the power feature input model is shown in Fig. 7. According to the statistical analysis of the confusion matrix, the model exhibits good recognition performance for incandescent lamps with lower power levels and vacuum cleaners with higher power levels. The power features of incandescent lamps and vacuum cleaners are completely different from those of other loads, which can be clearly reflected in the power signal. However, for other load types, the accuracy is relatively low due to variations in power consumption among different types and brands, with an average accuracy of around 0.4. Moreover, within the same category, the model struggles to distinguish between microwave ovens and laptops, which have similar power levels, resulting in poor recognition performance.

The confusion matrix for the recognition under the UI trajectory feature input model is shown in Fig. 8. The experimental setup was consistent with the previous ones. Overall, the UI trajectory model exhibits better recognition performance than the previous two models due to its rich image representation characteristics. In particular, it performs well in distinguishing between devices within the same category that have similar physical structures and power features, such as laptops and microwave ovens. However, there are still some misclassifications. According to the confusion matrix, a large number of laptops are mistakenly classified as CFLs, mainly due to the similarity in UI trajectories between individual models of these two types of devices. The same problem also arises between the two categories of fans and hair dryers. The F1 score for the recognition of CFLs and laptops is also only 0.62 and 0.55, respectively.

Finally, the local decision results obtained by inputting three parallel features into the models were fused by using the minimum Bayesian loss function, and the corresponding output confusion matrix results are shown in Fig. 9. From the confusion matrix, it can be observed that after decision fusion, the load recognition performance between different categories has reached an ideal state. The recognition accuracy for each category is above 0.95.

In conclusion, it can be observed that the model after undergoing decision fusion using the minimum Bayesian loss function, achieves the complementary advantages of the three representative features. For each type, the F1 scores for individual feature input recognition and recognition after decision fusion are shown in Table V. It is evident that the F1 scores for load identification of each device category have

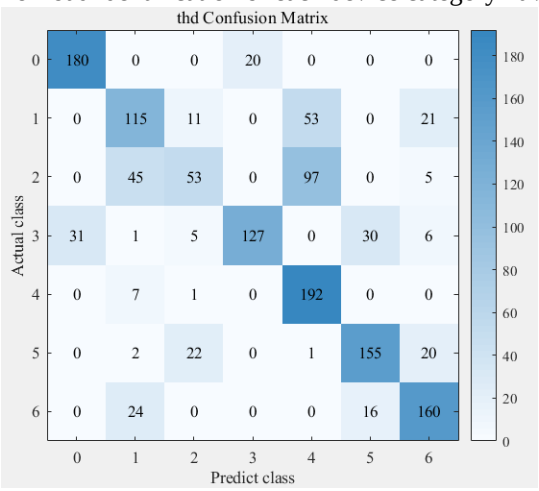

Fig. 6. Confusion matrices for samples under the THD feature.

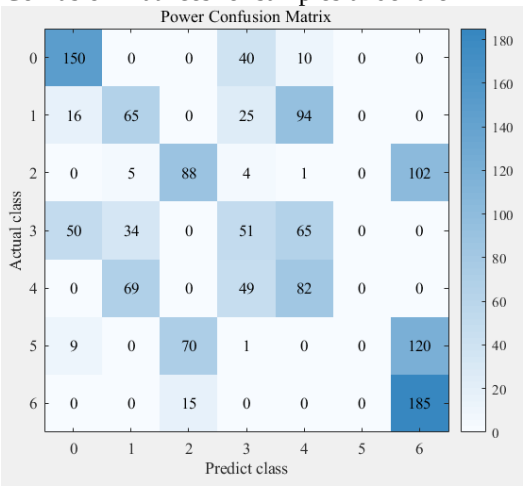

Fig. 7. Confusion matrices for samples under the power feature.

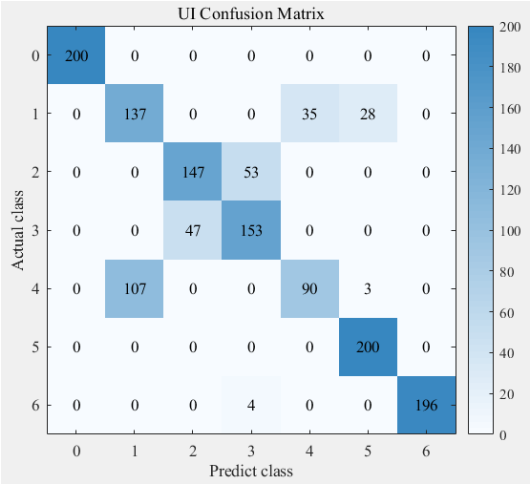

Fig.8. Confusion matrices for samples under the UI trajectory feature.

improved to above 0.95, with an average recognition accuracy of 0.98. This confirms the effectiveness of the proposed Softmax Bayesian decision fusion method for load identification.

Finally, the proposed method in this paper is compared with

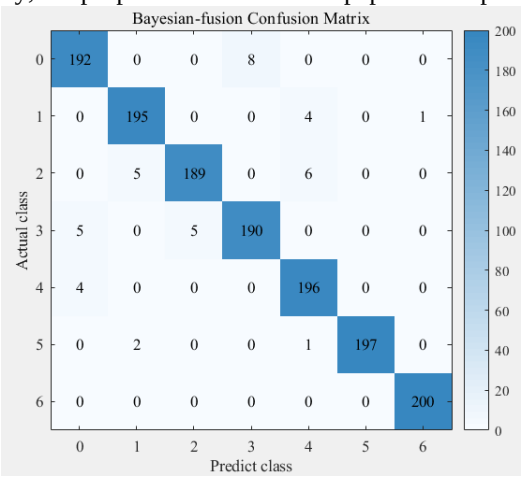

Fig.9. Confusion matrices for samples using Minimum Bayesian loss function decision fusion.

TABLE V

F1-SCORE COMPARED BETWEEN INDIVIDUAL FEATURE INPUT AND SOFTMAX BAYESIAN DECISION FUSION

	CFL	Hair-dryer	Elec-tric fan	Incande-scent lamp	Lap-top	Micro-wave oven	vacuum cleaner
UI trajectory	1	0.62	0.75	0.75	0.55	0.93	0.99
THD	0.88	0.58	0.36	0.73	0.71	0.77	0.78
Power	0.71	0.35	0.47	0.28	0.36	0	0.61
Decision Fusion	0.96	0.97	0.96	0.95	0.96	0.99	1

TABLE VI

F1-SCORE COMPARED WITH OTHER ALGORITHMS

	This study	[9]	[18]
CFL	0.96	1	0.92
Hairdryer	0.97	1	0.77
Electric fan	0.96	0.75	0.68
Incandescent lamp	0.95	1	0.89
Laptop	0.96	1	0.98
Microwave oven	0.99	1	0.98
Vacuum cleaner	1	1	0.00

existing models, and the comparative results are shown in Table VI. To ensure the effectiveness of the comparison, the selected comparative methods were validated using the publicly available PLAID dataset. Reference [21] utilizes the fusion of UI trajectory features and power features to form composite features, which are then inputted into a BP neural network for load identification. Reference [38] adopts a multilayer perceptron classifier based on the good additivity principle of UI trajectory and harmonic currents for load identification.

It can be inferred from Table VI that reference [21] exhibits poor performance in identifying fans, while reference [38] achieves good results in recognizing power electronic loads. However, reference [38] also struggles to accurately identify motor-driven loads such as fans, hair dryers, and vacuum cleaners. This indicates that the proposed algorithm in this study comprehensively considers the three major typical electrical features of the device categories in household loads. As a result, it demonstrates better robustness and achieves good recognition performance for diverse load types.

IV. CONCLUSION

To address the issue of diverse electrical characteristics and distinct load features among different types of electrical devices, this paper proposed a decision fusion identification method that incorporates three major representative features. Leveraging the innovative combination of an adaptive threshold CUSUM algorithm with Softmax-Bayesian decision fusion, this approach fills a gap in previous studies by providing a comprehensive solution for the accuracy of load identification in complex scenarios involving household appliances.

Firstly, an adaptive threshold CUSUM event detection method is proposed, which significantly addresses the issue of high-power event misjudgment and low-power event missed detection in existing change-point detection theory due to large power spans, and improves the F1 score to 0.866. Following this, a non-intrusive load identification method based on decision fusion Softmax-Bayesian is introduced, which simultaneously leverages the complementary advantages of THD (Total Harmonic Distortion), power, and UI trajectory features, overcoming the limitation of inaccurate identification of some components using a single load feature. Moreover, the integration of the adaptive threshold CUSUM algorithm with Softmax-Bayesian decision fusion achieves enhanced performance. Finally, the proposed method is

evaluated by using the publicly available PLAID dataset for household load sampling. By comparing the recognition performance of individual feature input models with that of decision fusion, and comparing the recognition performance of the proposed method with existing reference methods, the effectiveness of the proposed method is confirmed.

Experimental results conclusively demonstrate the efficacy of applying the proposed method to load identification across seven common household appliances, yielding an impressive average F1 score of 0.97. And for these seven types of appliances, the values of their F1 score were not less than 0.95. It underscores that the method demonstrates a high level of accuracy and reliability in practical applications. This can not only enhance the intelligence level of the power demand side but also offer a dependable solution for load identification in smart home systems or power management systems.

However, due to time and equipment constraints, there are still many shortcomings in this study that warrant further research and improvement. They are summarized as follows:

1)Expansion of the application scenarios for load identification: This study primarily focused on the types of household appliances and the analysis of their electrical features. The features of industrial and commercial loads were not considered. Further research is needed to explore the unique characteristics of industrial and commercial loads and develop identification features and methods suitable for them.

2)Model limitations in handling unknown load types: The method proposed in this study was designed for known common household load types, as it requires model training and the Softmax-Bayesian decision fusion method requires prior probability for decision-making. When encountering new load types that were not included in the model training, further research is needed to ensure the effectiveness of identifying unknown load types.

REFERENCES

[1] "IEEE guide for the benefit evaluation of electric power grid customer demand response," *IEEE Std 2030.6-2016*, vol., no., pp.1-42, 1Dec. 2016.

[2] Y. Zhou, S. Zhang, B. Ran, W. Yang, Y. Wang and X. Xiao, "Event-based two-stage non-intrusive load monitoring method involving multi-dimensional features," *CSEE J. Power Energy Syst.*, vol. 9, no. 3, pp. 1119-1128, May 2023.

[3] S. Makonin, F. Popowich, I. V. Bajić, B. Gill and L. Bartram, "Exploiting HMM sparsity to perform online real-time nonintrusive load monitoring," *IEEE Trans. Smart Grid*, vol. 7, no. 6, pp. 2575-2585, Nov. 2016.

[4] A. Tongta and K. Chooruang, "Long short-term memory (LSTM) neural networks applied to energy disaggregation," *2020 8th International Electrical Engineering Congress (iEECON)*, Chiang Mai, Thailand, 2020, pp. 1-4.

[5] P. Luo, X. Fan, J. Zhang and J. Li, "Non-intrusive load decomposition based on operation state of electrical appliances and deep learning," *Autom. Electr. Power Syst.*, Vol. 45, No. 12, Jun. 2021.

[6] P. A. Schirmer and I. Mporas, "Non-intrusive load monitoring: a review," *IEEE Trans. Smart Grid*, vol. 14, no. 1, pp. 769-784, Jan. 2023.

[7] K. D. Anderson, M. E. Bergés, A. Ocneanu, D. Benitez and J. M. F. Moura, "Event detection for non intrusive load monitoring," *2012 38th Annual Conference on IEEE Industrial Electronics Society (IECON)*, Montreal, QC, Canada, 2012, pp. 3312-3317.

[8] G. W. Hart, "Residential energy monitoring and computerized surveillance via utility power flows," *IEEE Technol. Soc. Mag.*, vol. 8, no. 2, pp. 12-16, Jun. 1989.

[9] J. Alcalá, J. Ureña, Á. Hernández and D. Gualda, "Event-based energy disaggregation algorithm for activity monitoring from a single-point sensor," *IEEE Trans. Instrum. Meas.*, vol. 66, no. 10, pp. 2615-2626, Oct. 2017.

[10] S. R. Shaw, S. B. Leeb, L. K. Norford and R. W. Cox, "Nonintrusive load monitoring and diagnostics in power systems," *IEEE Trans. Instrum. Meas.*, vol. 57, no. 7, pp. 1445-1454, Jul. 2008.

[11] C. Laughman et al., "Power signature analysis," *IEEE Power Energy Mag.*, vol. 1, no. 2, pp. 56-63, Mar.-Apr. 2003.

[12] A. U. Rehman, T. T. Lie, B. Vallès and S. R. Tito, "Event-detection algorithms for low sampling nonintrusive load monitoring systems based on low complexity statistical features," *IEEE Trans. Instrum. Meas*., vol. 69, no. 3, pp. 751-759, Mar. 2020.

[13] L. Niu and H. Jia, "Transient event detection algorithm for non-intrusive load monitoring," *Autom. Electr. Power Syst.*, vol. 35, no. 9, pp. 30-35, May 2011.

[14] H. Qu, J. Li, Z. Zhang, Z. Zhang and Q. Huang, "Study of Fast Identification Edge Detection Method for Electrical Equipment," *Proc. CSEE*., Vol.38, No.15, Aug. 2018.

[15] H. Chang, C. Lin and H. Yang, "Load recognition for different loads with the same real power and reactive power in a non-intrusive load-monitoring system," *2008 12th International Conference on Computer Supported Cooperative Work in Design(CSCWD)*, Xi'an, China, 2008, pp. 1122-1127.

[16] L. Du, D. He, R. G. Harley and T. G. Habetler, "Electric load classification by binary voltage–current trajectory mapping," *IEEE Trans. Smart Grid*, vol. 7, no. 1, pp. 358-365, Jan. 2016.

[17] M. Zhou, X. Song, J. Tu, G. Li, and K. Luan, "Residential electricity consumption behavior analysis based on non-intrusive load monitoring," *Power Syst. Technol.*, vol. 42, no. 10, pp. 3268-3276, Oct. 2018.

[18] Y. Lei, Z. Sun, Z. Ye and X. Wu, "Research on non-invasive load monitoring method in power system," *Trans. China Electrotech. Soc*., vol. 36, no. 11, pp. 2288-2297, Jun. 2021.

[19] J. Kang, M. Yu, L. Lu, B. Wang and Z. Bao, "Adaptive non-intrusive load monitoring based on feature fusion," *IEEE Sens. J.*, vol. 22, no. 7, pp. 6985-6994, Apr. 2022.

[20] H. Yin, K. Zhou and S. Yang, "Non-intrusive load monitoring by load trajectory and multi-feature based on DCNN," *IEEE Trans Industr Inform*, vol. 19, no. 10, pp. 10388-10400, Oct. 2023.

[21] S. Wang, L. Guo, H. Chen and X. Deng, "Non-intrusive load identification algorithm based on feature fusion and deep learning," *Autom. Electr. Power Syst.*, vol. 44, no. 9, pp. 103-110, May 2020.

[22] L. Zhang, T. Zhang, H. Zhang, F. Wang, and J. Guo, "Research on a method of load identification based on multi parameter hidden Markov model," *Power Syst. Prot. Control*, vol. 47, no. 20, pp. 81-90, Oct. 2019.

[23] R. Feng, W. Yuan, and L. Ge, "Non-intrusive load monitoring method for resident users based on alternating optimization in graph signal," *Proc. CSEE*, vol. 42, no. 4, pp. 1355-1365, Feb. 2022.

[24] J. Ling and Y. Peng, "Implementation of a non-intrusive load identification method based on event detection and CNN model," *Adv. Technol. Electr. Eng. Energy*, vol. 40, no. 3, pp. 46-54, Mar. 2021.

[25] C. Xu, K. Chen, J. Ma, J. Liu, and J. Wu, "Recognition of power loads based on deep belief network," *Trans. China Electrotech. Soc*., vol. 34, no. 19, pp. 4135–4142, Oct. 2019.

[26] H. Liu, S. Shi, X. Xu, D. Zhou, R. Min, and W. Hu, "A non-intrusive load identification method based on RNN model," *Power Syst. Prot. Control*, vol. 47, no. 13, pp. 162-170, Jul. 2019.

[27] H. Hwang and S. Kang, "Nonintrusive load monitoring using an LSTM with feedback structure," *IEEE Trans. Instrum. Meas.*, vol. 71, pp. 1-11, Apr. 2022.

[28] W. Ren and G. Xu, "Non-intrusive load decomposition method based on deep sequence translation model," *Power Syst. Technol*., vol. 44, no. 1, pp. 27-37, Jan. 2020.

[29] S. Zhang, Z. Zhu, B. Yin and X. Huang, "Event detection methods for nonintrusive load monitoring in smart metering: using the improved CUSUM algorithm," *2018 International Conference on Sensing, Diagnostics, Prognostics, and Control (SDPC)*, Xi'an, China, 2018, pp. 738-742.

[30] C. Truong, L. Oudre and N. Vayatis, " Selective review of offline change point detection methods, " *Signal Process.*, 2020.

[31]D. Shmilovitz, "On the definition of total harmonic distortion and its effect on measurement interpretation," *IEEE Trans. Power Del.*, vol. 20, no. 1, pp. 526-528, Jan. 2005.
[32]S. Huang, J. Xu, J. Ye and A. Shen, "Generalized Accurate Harmonic Calculation Method Based on Discretized Double Fourier Series to Solve Double-Pulse Phenomenon," *IEEE Trans. Ind. Electron*., vol. 70, no. 6, pp. 5651-5661, Jun. 2023.
[33]W. Yang, B. Chen, and L. Yu, "Bayesian-wavelet-based multisource decision fusion," *IEEE Trans. Instrum. Meas.*, vol. 70, pp. 1-10, Jul. 2021.
[34]J. Gao, S. Giri and E. C. Kara, "PLAID: a public dataset of high-resoultion electrical appliance measurements for load identification research: demo abstract," *Proceedings of the 1st ACM Conference on Embedded Systems for Energy-Efficient Buildings, Memphis Tennessee: ACM*, 2014: 198–199.
[35]Tieleman, T. and G. Hinton, "Neural networks for machine learning," *Lecture 6.5-RMSProp, COURSERA*, University of Toronto, Technical Report, 2012.
[36]X. Qiu, S. Yin, Z. Zhang, Z. Xie, M. Jiang and J. Zheng, "Non-intrusive load identification method based on V-I trajectory and high-order harmonic feature," *Electric Power Eng. Technol.*, vol. 40, no. 6, Nov. 2021.
[37]Y. Liu, X. Wang and W. You, "Non-intrusive load monitoring by voltage–current trajectory enabled transfer learning," *IEEE Trans. Smart Grid*, vol. 10, no. 5, pp. 5609-5619, Sept. 2019.
[38]D. Shmilovitz, "On the definition of total harmonic distortion and its effect on measurement interpretation," *IEEE Trans. Power Deliv.*, vol. 20, no. 1, pp. 526-528, Jan. 2005.